Effective and Mean Temperatures of a Cylindrical CSBA Loaded Fuel Pellet

Sunjoo Yoon [a] and Yonghee Kim [a]*
[a]*Korea Advanced Institute of Science and Technology, 291 Daehak-ro, Yuseong-gu, Daejeon 34141, Korea*
**Corresponding author: yongheekim@kaist.ac.kr*

1. Introduction

The effective temperature of a fuel pellet is a temperature such that if the entirety of the fuel was at that constant temperature, then the fuel pellet will have the same neutron multiplication factor as it does with a real temperature distribution.

Efforts to create a model for the effective temperature of uranium dioxide fuel pellets have been ongoing for decades and have produced various estimation methodologies, ranging from analytic estimates with a solid theoretical justification [1] to more empirical [2] methodologies. Generally, a simple volume-weighted average temperature is used.

Given a low rate of neutron absorption and some simplifying assumptions such as neglecting neutron scattering within the fuel cell, prior literature [3] suggests that the volume-weighted average temperature is a reasonable method of estimating the effective temperature of cylindrical fuel cells. If the rate of absorption is high, however, there is a stronger theoretical justification behind chord-averaged methods like the methodology suggested by Rowlands [1].

Most of these studies have been focused on cylindrical uranium dioxide (UO_2) fuel pellets as they are conventionally used in commercial nuclear power plants. However, as nuclear technology continues to develop, less conventional fuel geometries are being introduced. It is thus necessary to conduct further studies to address this issue.

One such effort to address this issue is a 2017 study on the effective temperature of a fuel cell design loaded with spherical centrally shielded burnable absorber, or CSBA, pellets by Rahman et al [4]. This study analysed the neutron multiplication factor (henceforth k_∞) of its CSBA-loaded fuel design across a range of burnups and found several tens of pcm in difference between the volume-weighted average and effective temperatures.

This investigation aimed to extend and generalise those findings by performing a similar study on a CSBA-loaded fuel cell with a different design, investigating the effective temperature of the fuel cell and the accuracy of a simple volume-weighted average in determining the effective temperature for several different burnup conditions.

2. Procedure

The overall structure of the investigation was as follows: first, a depletion analysis of the fuel was conducted to determine the material composition of the uranium dioxide and CSBA regions at MOC (25 MWd/kgU) and EOC (50 MWd/kgU) conditions. Then, multiphysics-coupled neutronics analyses were conducted for BOC, MOC, and EOC conditions to determine the neutron multiplication factor and fuel pellet temperature distributions. Finally, neutronics analyses assuming a flat temperature distribution were conducted for each of these conditions at a range of different temperatures. This was done to estimate the effective temperature of the fuel pellet and determine the discrepancy between the real neutron multiplication factor and the neutron multiplication factor of the flat temperature model with the average temperature.

All neutronics analyses were performed using the iMC code, a three-dimensional Monte Carlo-based stochastic neutronics simulation code [5]. It is generally considered good practice to use neutron interaction cross-section data for the highest available reference temperature not higher than the actual temperature being considered. However, all analyses in this investigation was performed using the built-in Doppler broadening model of the iMC code on cross-section data at 300 Kelvin in order to avoid issues arising from discontinuous interpolation between cross-sections at different temperatures.

2.1 Fuel Pellet Design

In this study, a cylindrical UO_2 fuel pellet surrounded by a helium gap and zircalloy cladding is modelled. Two cylindrical gadolinia CSBA pellets were placed along the centreline of the UO_2 region such that the distance between them was twice the distance between each and the axial pellet boundary. Since these fuel cells are axially stacked in an actual fuel rod, the distance between the two CSBA pellets in each cell would be equal to the distance between the top CSBA pellet in a given cell and the bottom CSBA pellet of the cell above it.

Table I: Basic information about the fuel pellet design

Pellet Geometry	
Radius, fuel region, cm	0.40958
Radius, cladding inner edge, cm	0.41873
Radius, cladding outer edge, cm	0.47600

Height, fuel pellet, cm	1.00000
CSBA pellets count	2.00000
Radius, CSBA pellet, cm	0.14000
Height, CSBA pellet, cm	0.12600
Pin pitch, cm	1.26230
Other Information	
Thermal Power, W	190.96500

This fuel pellet design is depicted in Figure 1.

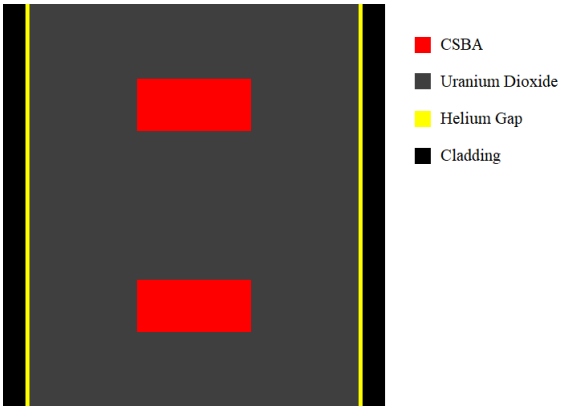

Fig. 1. Cross-section diagram of the fuel pellet design

2.2 Depletion Analysis

The depletion analysis of the fuel pellet was conducted using the built-in depletion function of the iMC code. The depletion analysis was perfomed in ten burnup steps up to 50 MWd/kgU. The calculations were performed using 100 inactive and 300 active cycles with 20,000 neutron histories for each burnup step.

This depletion analysis was conducted in six separate depletion regions within the fuel cell. The UO_2 fuel region was radially divided into three depletion regions. One depletion region represented the UO_2 closest to the centreline, one depletion region represented the region closest to the helium gap, and the third represented the region in between.

The gadolinia CSBA region was divided into three depletion regions of equal volume. One depletion region included both the axial and radial surfaces of both CSBA cylinders, one depletion region represented the centres of both CSBA cylinders, and the third depletion region was composed of the region between the surface and the central regions.

2.3 Multiphysics Analyses

The multiphysics module for the iMC code is capable of three-dimensional calculations using a tetrahedral mesh [6]. Thus, Gmsh [7] was used to subdivide the fuel pellet geometry into a mesh containing 39,090 tetrahedra to conduct the multiphysics-coupled analyses.

The same thermal conductivity formulas used by Rahman et al. were used for estimating the temperature- and burnup-dependent thermal conductivity of UO_2 fuel and the temperature-dependent thermal conductivity of the zircalloy cladding.

Preliminary investigations have revealed that the temperature distribution of the fuel pellet and its neutron multiplication factor converged to within stochastic uncertainties in just two or three iterations of thermal analysis. Thus, a multiphysics-coupled analysis was conducted with three thermal iterations for each burnup condition. The first two iterations were performed with 100 inactive and 300 active cycles with 50,000 neutron histories per cycle, and the final iteration was performed with 100 inactive and 1,200 active cycles with each cycle including 100,000 neutron histories.

2.4 Flat Temperature Analyses

Flat temperature neutronics analysis was performed at fuel temperatures varying from 600 to 1200 Kelvin in 100 Kelvin intervals for each of the three burnup conditions.

Since the real k_∞ value at each burnup condition was known from the multiphysics-coupled analysis, the effective temperature of the fuel cell at each burnup condition could be estimated by interpolating between the known k_∞ values over this range of temperatures. Each flat temperature analysis was conducted with 100 inactive and 1,200 active cycles, with 100,000 neutron histories per cycle.

Unlike in Rahman et al. [4], a flat-temperature analysis at the volume-weighted mean temperature was not conducted, as it was possible to estimate the corresponding k_∞ by interpolation between the results of the other flat-temperature analyses.

3. Results and Analysis

The neutron multiplication factors obtained by the analyses using the iMC code were tabulated below. The tabulated k_∞ values are unitless. The listed uncertainties represent one standard deviation of estimated stochastic variability in units of pcm. The results obtained from the multiphysics-coupled analysis at each burnup condition are listed as the reference value.

Table II: Neutron multiplication factor, BOC conditions

Reference	1.002844	±7.4
700K	1.006344	±7.3
800K	1.003718	±7.0
900K	1.000984	±7.5
1000K	0.998688	±7.2
1100K	0.996399	±7.3
1200K	0.994263	±6.9

Table III: Neutron multiplication factor, MOC conditions

Reference	0.979310	±6.9
700K	0.985037	±6.8
800K	0.981812	±6.8
900K	0.978845	±6.9
1000K	0.976020	±6.9
1100K	0.973235	±6.8
1200K	0.970729	±6.5

Table IV: Neutron multiplication factor, EOC conditions

Reference	0.952446	±6.8
700K	0.960295	±6.9
800K	0.956662	±7.0
900K	0.953518	±6.9
1000K	0.950306	±7.1
1100K	0.947420	±7.0
1200K	0.944610	±6.8

Figure 2, below, shows the neutron multiplication factors of the flat temperature analyses corresponding to the temperature at BOC, MOC, and EOC conditions. Second-order polynomial regression was found to fit the data well, as shown in Figure 2.

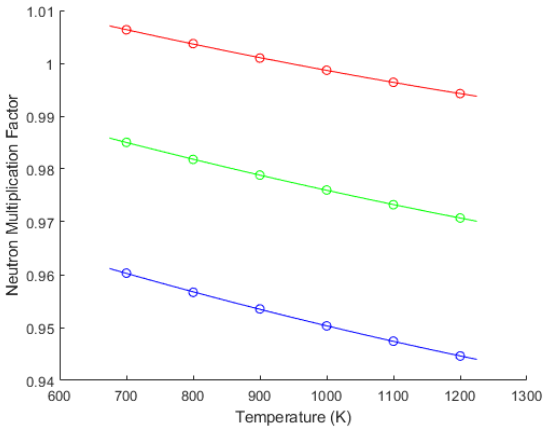

Fig. 2. Neutron multiplication factor by temperature; BOC in red, MOC in green, EOC in blue

The temperature distribution within the fuel pellet, at BOC conditions, is presented in Figure 3. Diagrams of the temperature distributions for the other burnup conditions are omitted, as these were not visually distinct from BOC conditions other than having a considerably higher centreline temperature and thus a stronger temperature gradient across the UO_2 fuel region. It may be noted that, unlike in conventional cylindrical fuel cells, the temperature is not axially constant but is rather higher in the uranium dioxide fuel region compared to the gadolinia CSBA region near the centreline. This is likely because the gadolinia CSBA have the effect of suppressing neutron flux in and around them and because less fission heat is generated in the CSBA regions than in the UO_2 regions.

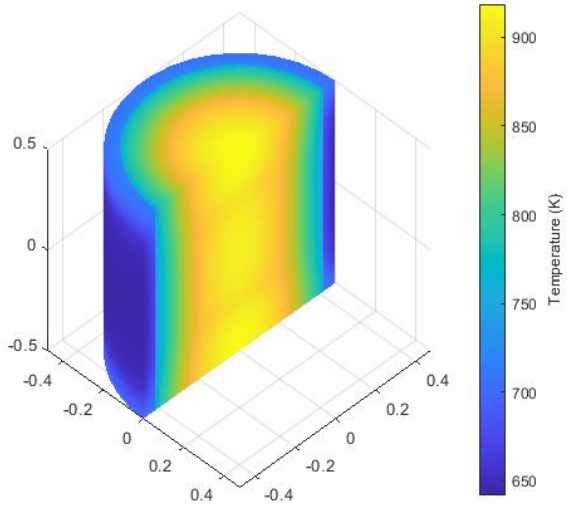

Fig. 3. Temperature distribution within the fuel pellet at BOC depletion conditions

From these temperature distributions, the fuel's centreline, surface, and average temperatures were calculated. The average temperature was calculated by taking the volume-weighted mean temperature of the fuel and CSBA regions. In a CSBA-loaded fuel cell, as the temperature varies axially, there are no single fuel centreline and surface temperatures and so similar, length-weighted or area-weighted averages were taken.

As mentioned previously, the actual k_∞ values of this fuel pellet at various burnup conditions and the lines of best fit interpolating the flat-temperature neutron multiplication factor by the fuel temperature were calculated. It was thus possible to estimate the effective temperature of the fuel pellet at BOC, MOC, and EOC conditions. Similarly, it is possible to estimate the flat-temperature neutron multiplication factors at the volume-weighted average fuel temperatures.

Many existing methods of estimating the effective temperature of uranium dioxide fuel pellets involve taking a weighted average of the fuel centreline and surface temperatures. Therefore, the appropriate weights necessary to obtain the effective temperature for this fuel cell were calculated. Since the two weights always sum to unity, the weights given to the surface were omitted from the results and only the weights given to the centreline are presented.

The results of this analysis are presented in Tables V to VII. The coefficients for the polynomial line of best fit are presented in descending order (that is to say, the quadratic coefficient first). The fuel temperature coefficient was obtained by evaluating the derivative of the polynomial line at the average temperature.

Table V: Key statistics of the pellet at BOC conditions

Coefficients, Polynomial regression	7.5536×10^{-9} K^{-2} -3.8540×10^{-5} K^{-1} 1.029641
Fuel temperature coefficient	–3.22 pcm K^{-1}
Temperature, average	834.55 K
Temperature, centreline	919.92 K
Temperature, surface	754.18 K
Temperature, effective	830.50 K
Centreline weight	0.4605
k_∞, Flat average temperature	1.002739
k_∞, Reference	1.002844
k_∞ discrepancy	10.5 pcm

Table VI: Key statistics of the pellet at MOC conditions

Coefficients, Polynomial regression	7.7196×10^{-9} K^{-2} -4.3266×10^{-5} K^{-1} 1.011524
Fuel temperature coefficient	–3.64 pcm K^{-1}
Temperature, average	892.73 K
Temperature, centreline	1037.63 K
Temperature, surface	754.44 K
Temperature, effective	883.97 K
Centreline weight	0.4574
Multiplication factor, Flat average temperature	0.979051
k_∞, Reference	0.979310
k_∞ discrepancy	25.9 pcm

Table VII: Key statistics of the pellet at EOC conditions

Coefficients, Polynomial regression	9.1911×10^{-9} K^{-2} -4.8710×10^{-5} K^{-1} 0.989846
Fuel temperature coefficient	–4.00 pcm K^{-1}
Temperature, average	951.01 K
Temperature, centreline	1155.48 K
Temperature, surface	754.61 K
Temperature, effective	931.57 K
Centreline weight	0.4415
k_∞, Flat average temperature	0.951835
k_∞, Reference	0.952446
k_∞ discrepancy	61.1 pcm

It may be noted that the centreline weights calculated for this fuel pellet are very similar to the 4/9 proposed by Rowlands [1] for cylindrical fuel cells and not similar to the 0.3 proposed by Finnemann and Galati [2]. Furthermore, the k_∞ discrepancies between the flat average temperature and the multiphysics-coupled models were on the order of several tens of pcm.

4. Conclusion

The difference between the actual k_∞ value and the flat average temperature k_∞ value was well within uncertainties at BOC conditions. However, this discrepancy was increased to 61 pcm for heavily depleted fuel. This result agrees with prior research conducted by Rahman et al. and are most likely generalisable to other CSBA-loaded fuel cells of similar design principles.

Expressing the effective temperature as a weighted average of the centreline and surface temperatures yield weights very similar to those proposed by Rowlands in 1962. The actual temperatures deviate from his 4/9 centreline and 5/9 surface weighted average method by no more than four Kelvin. This suggests that his proposal for cylindrical fuel cells may also be a reasonable method for estimating the effective temperature of CSBA-loaded fuel cells. Further research, however, may be needed to evaluate the generalisability of this conclusion for other CSBA-loaded fuel pellets designs.

ACKNOWLEDGEMENTS

This work was supported by the National Research Foundation of Korea (NRF) Grant funded by the Korean Government (MSIP) (NRF-2016R1A5A1013919)

REFERENCES

[1] G. Rowlands, “Resonance absorption and non-uniform temperature distributions”, *Journal of Nuclear Energy* Parts A and B, Vol. 16, pp. 235, 1962.
[2] H. Finnemann and A. Galati, “NEACRP 3-D LWR Core Transient Benchmark Final Specifications”, OECD Nuclear Energy Agency, 1992.
[3] W. de Kruijf and A. Janssen, “The Effective Fuel Temperature to Be Used for Calculating Resonance Absorption in a $^{238}UO_2$ Lump with a Nonuniform Temperature Profile”, *Nuclear Science and Engineering*, Vol. 123, No. 1, pp. 121-135, 1996.
[4] A. Rahman, X. Nguyen, and Y. Kim, “A Study on Effective Temperature of CSBA-loaded UO2 Fuel Pellet”, *Transactions of the Korean Nuclear Society Autumn Meeting*, 2017.
[5] H. Kim and Y. Kim, “Unstructured Mesh-Grid Multi-Physics Analysis with Monte Carlo iMC Code for Advanced Fuel Elements”, *Transactions of the American Nuclear Society*, Vol. 122, No. 1, pp. 738-741, 2020.
[6] H. Kim and Y. Kim, “Unstructured Mesh-Based Neutronics and Thermomechanics Coupled Steady-State Analysis on Advanced Three-Dimensional Fuel Elements with Monte Carlo Code iMC”, *Nuclear Science and Engineering*, Vol. 195, No. 5, pp. 464-477, 2020.
[7] C. Geuzaine and J.-F. Remacle, “Gmsh: a three-dimensional finite element mesh generator with built-in pre- and post-processing facilities”, *International Journal for Numerical Methods in Engineering*, Vol. 79, No. 11, pp. 1309-1331, 2009.